

Review

On the Behaviour of Living Cells under the Influence of Ultrasound

David M. Rubin, Nicole Anderton, Charl Smalberger, Jethro Polliack, Malavika Nathan and Michiel Postema *

School of Electrical and Information Engineering, University of the Witwatersrand, Johannesburg, 1 Jan Smuts Laan, 2050 Braamfontein, South Africa; david.rubin@wits.ac.za (D.M.R.); 673663@students.wits.ac.za (N.A.); 2026923@students.wits.ac.za (C.S.); jethro.polliack@students.wits.ac.za (J.P.); malavika.nathan@students.wits.ac.za (M.N.)

* Correspondence: michiel.postema@wits.ac.za; Tel.: +27-11-7177237

Received: 19 September 2018; Accepted: 22 October 2018; Published: 26 October 2018



Abstract: Medical ultrasound technology is available, affordable, and non-invasive. It is used to detect, quantify, and heat tissue structures. This review article gives a concise overview of the types of behaviour that biological cells experience under the influence of ultrasound only, i.e., without the presence of microbubbles. The phenomena are discussed from a physics and engineering perspective. They include proliferation, translation, apoptosis, lysis, transient membrane permeation, and oscillation. The ultimate goal of cellular acoustics is the detection, quantification, manipulation and eradication of individual cells.

Keywords: cellular acoustics; ultrasound-induced lysis; acoustic microparticle manipulation; ultrasound-induced cell translation; micro-acoustics; non-bubble-assisted sonoporation

1. Introduction

Ultrasound technology is available, affordable and non-invasive. Therefore, it finds widespread application in medicine. Ultrasound is well established as an imaging modality in medical diagnostics, and, more recently, its use has been extended to therapy. Ultrasonic therapeutic modalities in current clinical practice are high-intensity focussed ultrasound (HIFU) [1], extracorporeal shockwave lithotripsy [2], ultrasound contrast agent-assisted drug delivery [3], and combinations of some of these modalities [4]. Acoustic cluster therapy has shown great promise in a mouse study [5]. The aforementioned therapeutic modalities [1–5] are directed at modifying the macro-structural aspects of tissue. Claims have been made about pain relief with the aid of ultrasound equipment, but these are not supported by scientific evidence [6,7]. Several studies have suggested increased tissue repair owing to ultrasound exposure [8,9], which has led to the increased use of ultrasound equipment when treating bone fracture [10]. However, the acoustic setups of these [8–10] and other [11–14] tissue-repair studies have been such that thermal effects could not be ruled out. In fact, heating is the most plausible explanation for the phenomena observed [15]. The emerging field of ultrasonic manipulation at the micro-structural level, i.e., the individual cellular level, holds great promise both in diagnostics and therapeutics, and will constitute the focus of this review article.

The vast majority of scientific publications on the response of biological cells to ultrasound involve bubbles. Reviews on bioeffects typically do not include the situations without ultrasound contrast agents or inertial cavities [16–19]. This article reviews those effects of ultrasound on living cells that do not include inertial cavitation, cellular effects due to the introduction of bubbles, and non-destructive structural evaluation through ultrasonic biomicroscopy.

As an introduction to the topic, a simple model of the cell is assumed, followed by a brief summary of the relevant ultrasound parameters. The paper then covers various studies on the effects of ultrasound on cells. The cell types covered in these studies include plant cells, bacteria, cancer cells, mammalian cells, red blood cells, and platelets.

1.1. Cells

Cells are ubiquitous in living organisms, with the adult human body containing more than 10^{14} of these complex structures [20]. Knowledge of the mechanical properties of cells is essential to appreciate their behaviour in response to ultrasound.

Cells have a wide variety of morphological characteristics, and in mammals they typically range in diameter from 6 μm to 40 μm . While cells are complex structures, for the purpose of understanding cellular acoustics, a simplified model is assumed, shown in Figure 1.

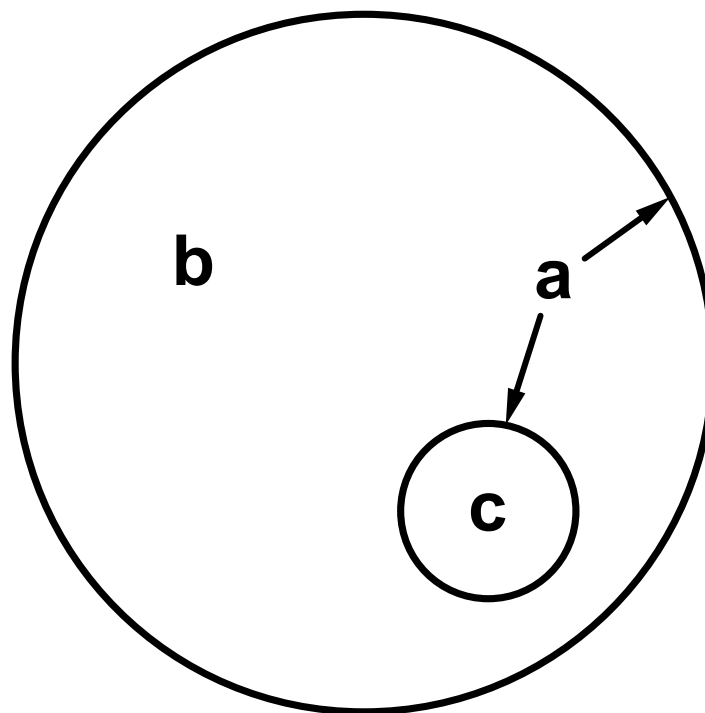


Figure 1. Highly simplified schematic of a standard mammalian cell, with bilayer membranes (a) surrounding the cell and the nucleus; cytoplasm (b); and a nucleus (c).

The external surface of all cells is a semi-permeable lipid-based membrane. This so-called plasma membrane is the cell's elastic surface that separates the cell's gel-like fluid, known as cytoplasm, from its external surroundings. Cell membranes are gelatinous structures which play a role in cellular processes such as growth, movement, division and secretion. The number of double bonds in the organic compounds of the plasma membrane affects the fluidity of the membrane, with more double bonds correlating to increased fluidity [20].

The cytoplasm consists of all the material inside of a living cell, with the exception of the nucleus [20]. With a bulk modulus of 4 TPa, the incompressible cytoplasm facilitates the cell's ability to elongate, but not to shrink [21]. This means that cells deform when subjected to compressive forces. Some cells, particularly plant cells, have an additional rigid, cellulose-based, outer wall for structural support. Located within the cytoplasm are a range of sub-cellular structures known as organelles. While not found in all cells, the nucleus, if present, contains the genetic material which directs cellular function.

Damaged cells contribute towards life-threatening diseases, making it advantageous to remove these cells from human and animal bodies [22]. Damaged cells are naturally separated from healthy cells and then destroyed by the body’s internal mechanisms, e.g., apoptosis. Techniques have been developed to separate cells; these techniques are mostly based on adherence, density, and antibody binding [22]. The most common in-vitro density-based method is centrifugation, which is an expensive and tedious method. There is a need for a cost-effective, efficient method to remove damaged cells, not only in vitro, but also in vivo—from the human body.

1.2. Ultrasound

In medical ultrasonics, ultrasound fields are generated with multi-element transducers, called probes [23]. There are many differences in probe geometry and signal output, contributing to a vast number of radiated ultrasound fields [24]. An ultrasound field at a specific location is characterised by its dominant period, centre frequency, pulse length, peak-negative pressure, peak-positive pressure, peak-to-peak pressure, pulse-repetition time, pulse-repetition frequency, and duty cycle [25]. These parameters are schematically shown in Figure 2. The dominant period is the time taken to complete a single sonic cycle. The centre frequency is the inverse of the dominant period. The pulse length is the duration of pulse transmission. The pressure amplitude p_A may vary within a pulse. Consequently, the pulse pressure is typically expressed in its peak-positive, peak-negative, and peak-to-peak pressures. The pulse-repetition period is the duration from the onset of a pulse to the onset of the next pulse. The pulse-repetition frequency is the inverse of the pulse-repetition period. The duty cycle is the percentage of transmission time during a pulse sequence.

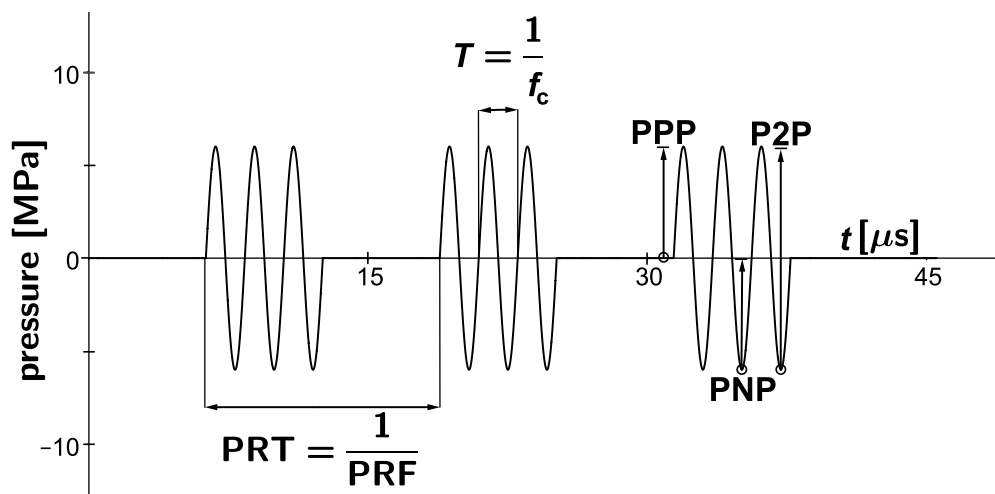


Figure 2. Representation of an ultrasound pulse sequence with dominant period T , centre frequency f_c , peak-positive pressure (PPP), peak-negative pressure (PNP), peak-to-peak pressure (P2P), pulse-repetition period (PRT), and pulse-repetition frequency (PRF).

The power W is by definition the transmitted energy per unit time. Every point in a sound field lies on a surface S on which the intensity $I = W S^{-1}$ is the same. The average intensity is given by [25]:

$$\langle I \rangle = \frac{p_A^2}{2\rho c}, \tag{1}$$

where p_A is the acoustic pressure amplitude, c is the speed of sound of the medium and ρ is the density of the medium.

It should be noted that, in medical ultrasonics, the bulk of the acoustic waves propagate through the human body, whilst only a small portion is scattered on tissue transitions and micro-structures [25].

Although ultrasound is by definition all sound with frequencies greater than 20 kHz, for most medical applications, including physiotherapy [26], ultrasound devices with frequencies greater

than 500 kHz are used. Ultrasound with frequencies of 10–100 MHz is used for biomicroscopy [27], i.e., the non-destructive evaluation of cellular structures [28]. Biomicroscopy does not involve the active response of cells and is therefore excluded from this review.

If the peak-negative acoustic amplitude surpasses a critical threshold, the so-called cavitation threshold, bubbles may form in a liquid [23,29–31]. Inertial cavitation has been associated with the formation of free radicals [32,33], causing harmful biological effects [34,35] but also with applications in drug delivery [36]. These so-called bioeffects have been studied since 1928 [37,38].

An indication of potential mechanical damage due to inertial cavitation is given by the mechanical index (MI):

$$MI = \frac{PNP}{\sqrt{f_c}}, \quad (2)$$

where peak-negative pressure (PNP) is expressed in MPa and f_c is expressed in MHz. The value taken for PNP should be the maximum anywhere in the field, measured in water but reduced by an attenuation of $0.3 \text{ dB cm}^{-1} \text{ MHz}^{-1}$.

For mechanical index values between 0.3 and 0.7, slight damage to the neonatal soft tissues such as the lung or intestine may occur [39], whereas ultrasound applied with a mechanical index value greater than 0.7 is considered unsafe for diagnostic applications [40,41]. Mechanical indices have been limited to 1.9 for medical imaging with commercial scanners [42]. A mechanical index of less than 0.3 is recommended for medical diagnostic applications [23].

Although the ultrasound-assisted formation of bubbles in the body is regarded as damaging, and therefore often unwanted, phenomenon *in vivo*, artificial microbubbles have been injected for diagnostic purposes. These so-called ultrasound contrast agents consist of encapsulated microbubbles with diameters below $6 \mu\text{m}$. The microbubbles oscillate, translate, ripen, coalesce, jet, and cluster under the influence of ultrasound [43]. At low MI, their characteristic acoustics make them suitable tracers for perfusion imaging [44]. At high MI, they act as cavitation nuclei, amplifying effects of inertial cavitation. The damaging effects of inertially driven bubbles on cells have been studied intensively [45]. It is however, beyond the scope of this review paper, as its focus is on the influence of ultrasound itself on biological cells.

In the case of bubble presence, the ultrasound predominantly acts to activate the bubbles to interact with the nearest structure, which just may happen to be a biological cell [17]. Studying the interactions of acoustically active bubbles near cells is a field on its own, with the primary purpose of understanding sonoporation [46,47]. Sonoporation is the transient permeation and resealing of a cell membrane with the aid of ultrasound, typically but not necessarily in the presence of an ultrasound contrast agent. Sonoporation allows for the trans-membrane delivery and cellular uptake of macromolecules [48] between 10 kDa and 3 MDa [49], and is therefore of utmost interest for ultrasound-aided drug [50] and gene delivery [51]. Although the mechanical disruption with the aid of ultrasound has been attributed to damaging effects of inertial cavitation [52–55], the increased uptake has also been observed, albeit less frequently, at low acoustic amplitudes, i.e., in acoustic regimes where inertial cavitation is not to be expected and without the presence of microbubbles [56]. Consequently, the studies on sonoporation without the presence of microbubbles have been included in this review, if the acoustic regime applied was below the inertial cavitation threshold. Sonoporation studies with probable microbubble presence have been excluded from this review.

1.3. Mechanical Cell Response to Ultrasound

Let us modify the cell model of Figure 1 to a model with an incompressible nucleus, shown in Figure 3, with the bilayer cell membrane of inner radius R_1 and outer radius R_4 split into an outer monolayer membrane of thickness $(R_4 - R_3)$ and an inner monolayer membrane of thickness $(R_2 - R_1)$, separated by a gaseous void of thickness $(R_3 - R_2)$. It is assumed that $(R_3 - R_2) \ll (R_4 - R_3) = (R_2 - R_1)$ [57,58].

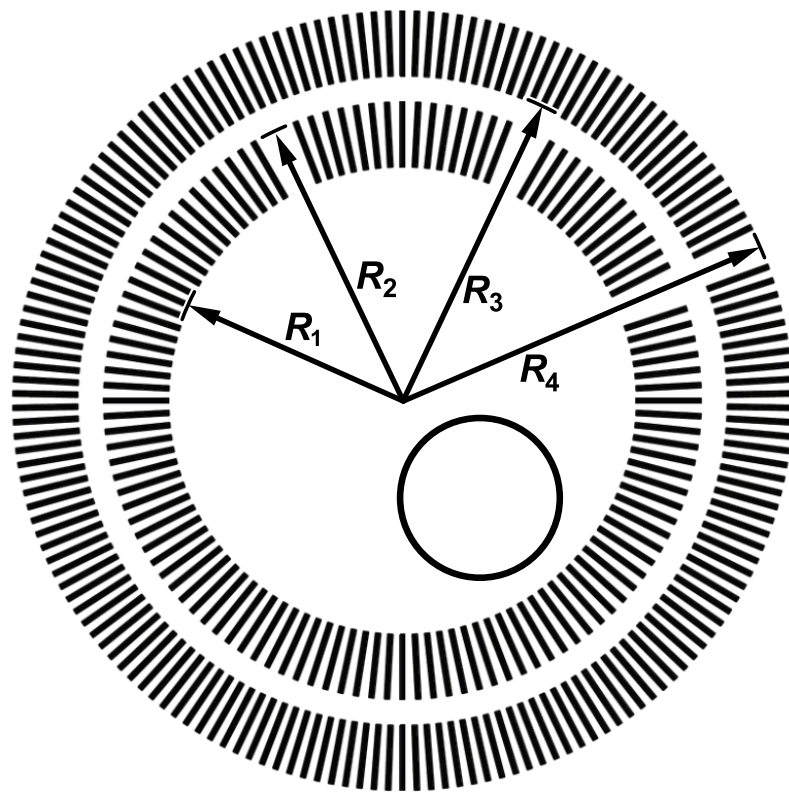


Figure 3. Highly simplified schematic of a cell with an outer monolayer membrane of thickness $(R_4 - R_3)$ and an inner monolayer membrane of thickness $(R_2 - R_1)$, separated by a gaseous void of thickness $(R_3 - R_2)$.

The oscillation dynamics of a spherically symmetric cell with incompressible nucleus an outer Newtonian membrane of finite thickness, surrounded by a Newtonian viscous liquid, are governed by a Rayleigh–Plesset-like equation of the following form [57]:

$$\begin{aligned} \rho R_3 \ddot{R}_3 \left[1 + \left(\frac{\rho - \rho_M}{\rho_M} \right) \frac{R_3}{R_4} \right] + \rho \dot{R}_3^2 \left[\frac{3}{2} + \left(\frac{\rho - \rho_M}{\rho_M} \right) \left(\frac{4R_4^3 - R_3^3}{R_4^3} \right) \right] \\ = p_{g0} \left(\frac{R_{30}^3 - R_2^3}{R_3^3 - R_2^3} \right)^\gamma - \frac{2\sigma_3}{R_3} - \frac{2\sigma_4}{R_4} - p_0 - P(t) - 4\eta \frac{R_3^2}{R_4^3} \dot{R}_3 - 4\eta_M \frac{R_4 - R_3}{R_3 R_4^3} \dot{R}_3, \end{aligned} \quad (3)$$

where R_n is the instantaneous radius of membrane interface n (cf. Figure 3), ρ_M is the membrane density, p_{g0} is the initial gas pressure inside the void, R_{30} is the initial radius of interface 3, γ is the polytropic exponent of the gas inside the void, σ_n are the surface tensions at the two respective interfaces n of the outer membrane, p_0 is the ambient pressure, $P(t)$ is the acoustic driving pressure as a function of time, η is the viscosity of the medium, and η_M is the membrane viscosity.

Numerical solutions of Equation (3) have shown that, even at low acoustics amplitudes, the void inside the bilayer membrane may have oscillation amplitudes of multiple times its initial thickness. Although these excursions are not enough to permanently damage a human cell [57], they are strong enough to induce physical translation of the cell. To turn bilayer membranes into inertial cavities, acoustic amplitudes would be required greater than the inertial cavitation threshold [57].

A general one-dimensional translation equation for a cell with an incompressible liquid core surrounded by a compressible void subjected to a spatio-temporal pressure field $P(x, t)$ has been derived [59]:

$$m_C \ddot{x} + \frac{2\pi}{3} \rho \frac{d}{dt} (R_4^3 \dot{x}) = -\frac{4\pi}{3} R_4^3 \frac{\partial}{\partial x} P(x, t) + F_d, \quad (4)$$

where m_C is the mass of the cell and F_d is the drag force [60].

To summarise numerical studies on cell translation—in a standing ultrasound field, cells may move to nodes or antinodes of the sound field, owing to primary Bjerknes forces [61,62]. In addition, cells might attract each other, owing to secondary Bjerknes forces. The collision speed of two identical oscillators subjected to mutual secondary Bjerknes forces is proportional to the oscillator size to the power of five and inversely proportional to the squared distance between the oscillators [43]. Given the small volume of the gaseous voids inside cell membranes, the oscillation excursions at safe ultrasound pressures might not be high enough for biological cells to create secondary Bjerknes forces strong enough to attract other cells, unless the cells are already very close to each other. However, Henrietta Lacks (HeLa) cells have been reported to attract ultrasound contrast agent at a low mechanical index, which Delalande et al. attributed to secondary Bjerknes forces [56,63].

2. Overview of Scientific Publications on Cellular Ultrasonics

The following overview of scientific publications on cellular ultrasonics excludes papers on high-intensity focussed ultrasound (HIFU), microbubble-assisted sonoporation, and inertial cavitation. However, in some papers that deal with ultrasound-cell interaction, the acoustic regime has not been properly stated, making the experiments non-repeatable [64] and occasionally implausible [65]. In cases where there was some cause for doubt whether inertial cavitation played a role, it was chosen to include these papers.

2.1. Early Studies

It was chosen to include a few of the earliest papers on cellular acoustics out of historic curiosity, although the acoustic regimes of these papers are most probably beyond the inertial cavitation threshold. The articles in this section are in chronological order.

In a 1964 study, newt larvae were subjected to 5 min of 1 MHz ultrasound at intensities of 8–15 W cm⁻² [66]. Their notochord cells appeared normal on light microscopy, but the endoplasmic reticulum was seen to be severely disrupted on electron microscopy. By 24 h post sonication, 50% of the endoplasmic reticulum had reverted to a normal structure.

In an early study on chromosome aberrations induced by ultrasound, two commercial foetal ultrasound devices were used [67]. Cultured healthy-donor blood was subjected to ultrasound for 1- and 2-h durations using these devices with manufacturer specifications of 2.25 MHz and maximum power of 30 mW. The cultured cells were examined for chromosomal aberrations after sonication. There was clear evidence of substantially increased chromosomal damage in the sonicated samples compared to controls. In addition, the longer duration produced greater damage. No formal statistical significance test was reported on the results.

As an early study on bioeffects in tissue [68], frog muscle was subjected to sonication at 85 kHz using a vibrating needle machined into a stainless steel acoustic horn. The sound amplitude was expressed in terms of the deviation of the needle tip which ranged from 1–5 μm, with maximum deviation corresponding to a sub-cavitation pressure amplitude of 0.125 atm. The temperature rise was minimal and, at low amplitudes, structures such as the mitochondrial cristae showed disruption. At higher amplitudes, disruption to the Z and M lines was demonstrated. Z and M lines are anatomical structures that are evident on microscopy and that relate to the organisation of actin and myosin protein filaments in muscle cells. Actin and myosin are proteins responsible for muscle contraction. The data suggest that the degree of disruption is dependent on duration and amplitude of sonication. These effects were seen after 1 min of sonication. The minimal temperature rise and the sub-cavitation pressure amplitudes suggest a mechanism other than cavitation and thermal effects for the cell disruption. The authors speculate that the changes may be due to acoustic streaming and movement due to radiation forces. They point out that the relatively constrained structures in muscle cells are not expected to be subjected to these forces. However, in the presence of non-uniform sound fields, twisting and stretching of the membranes and filamentous structures may occur, due to viscous stresses.

In succession of studies on plant cells by M.W. Miller [69,70], D.G. Miller subjected *Elodea* cells to ultrasound for 100 s at frequencies ranging from 0.45 to 10 MHz [71]. Intensity thresholds for cell death were found to vary with frequency and ranged from 75 mW cm^{-2} at 0.65 MHz to 180 mW cm^{-2} at 5 MHz. Cell death was attributed to the presence of gas bodies in inside the *Elodea* leaves, modelled in a separate paper [72]. The ultrasound-induced motion of fluids had been reported earlier inside *Elodea* leaves [73] and in a *Curcubita pepo* hair cell [74].

Discoid platelet suspensions were subjected to ultrasound fields in the 1–10-MHz frequency range at acoustic pressure amplitudes in the range of 0.5–76 kPa [75]. Acoustic streaming was observed and changes in transmitted light intensity were attributed to changing platelet orientation. Platelet disruption had been reported after 5 min of 1-MHz sonication at intensities of 0.2 and 0.6 W cm^{-2} [76]. In the latter study, following sonication, platelet debris were observed and platelet function was impaired. There were qualitative differences between sonicated and non-sonicated specimens in the macroscopic characteristics of the clot.

This concludes the overview of early cellular acoustics studies. Despite the high intensities used, not all phenomena observed are destructive, most notably intracellular streaming.

2.2. Damage

This section gives an overview of cellular acoustics studies that resulted in transient or permanent cell damage. The studies have been treated in chronological order.

Human red blood cells were put in dialysis tubing and exposed to 1 to 2 min of 1-MHz continuous-wave ultrasound at intensities of $0\text{--}5 \text{ W cm}^{-2}$ spatial peak temporal average [77]. Some of the samples contained ultrasound contrast agent. The degree of cell lysis was found to be intensity-dependent. The maximum lysis was over 50% with ultrasound contrast agent present and 30% without ultrasound contrast agent at an intensity of 3 W cm^{-2} . After this maximum, with increasing intensity, there was some decline in lysis. The degree of lysis was found to be insensitive to the concentration of ultrasound contrast agent but decreased with increasing red blood cell concentrations (haematocrit).

Rendering cell membranes permeable to large molecules such as proteins and deoxyribonucleic acid (DNA) has potential therapeutic applications [78]. The effects of ultrasound on cell membrane permeation was studied by subjecting bovine red blood cells to continuous ultrasound at 24 kHz. A number of incident pressures were used in this study under various conditions and were estimated to range from less than 1 atm to 10 atm. Permeation was determined by measuring the haemoglobin released, which was found to increase as a linear function of incident pressure. It was also found to increase as a function of sonication time, with a threshold for permeation of 100 ms.

A human leukaemia-60 (HL-60) cell line in suspension was exposed to continuous-wave 255-kHz ultrasound at an intensity of 0.4 W cm^{-2} for 30 s [79]. Experiments were performed with and without the photosensitive drug merocyanine 540. Scanning electron microscopy showed that, in the presence of merocyanine 540, there were substantial disruptions to the cell membrane including porosity, dimpling craters, and breaches. In the absence of the drug, however, minimal membrane changes were observed. In addition, inclusion of merocyanine 540 in the ultrasound experiments resulted in a measurable diminution in cell viability which was not seen in the absence of the drug. This study is the reason that sonic cell permeation is referred to as sonoporation.

Belgrader et al. investigated the effect of ultrasound sonication on the spore-forming bacterium *B. subtilis*, which served as an anthrax spore (*B. anthracis*) surrogate [80]. The study aimed at identifying suitable techniques to disrupt anthrax spores, a critical step in achieving rapid and sensitive genetic identification, e.g., polymerase chain reaction (PCR), in cases where *B. anthracis* spores are used as a weapons. These spore-forming bacteria have an outer cortex that is extremely resistant to disruption (lysis) by various physical and chemical techniques, and the goal was to identify a technique that could achieve rapid spore lysis. Spore disruption was achieved by incubating the spores with 106- μm glass beads to enhance the destructive effects of cavitation. Sonication using 60 W at 67 kHz for 2 min,

50 W at 22 kHz for 30 s, and 40 W at 47 kHz for 30 s were tested. In their final design, adequate cell lysis was achieved in 30 s.

In a follow-up study [81], spores of the same bacterium *B. subtilis* were subjected to sonication at 40 kHz in the presence of 106- μm glass beads for 10 to 20 s. The acoustic horn amplitudes used were expressed in its surface displacement, 25 and 38 μm peak-to-peak, and the sonicated liquid was subjected to hydrostatic pressures ranging from 34 to 138 kPa, in an attempt to improve coupling between the horn and the liquid. The ultrasonic energy was transferred from the horn to the fluid via a thin flexible membrane and it was shown that this design avoids cavitation as large pressure drops were absent due to the film separating from the horn. The sonication technique produced effective disruption of bacterial spores as evidenced by scanning electron microscopy. The utility of this technique as a means of releasing DNA from disrupted spores for the purpose of molecular diagnostics was discussed and it was concluded that the efficiency of DNA amplification using PCR increased as a function of the applied hydrostatic pressure.

In a leukaemic cell study [82], therapeutic ultrasound at a frequency of 750 kHz and spatial-peak temporal average intensity levels of 103.7 W cm^{-2} and 54.6 W cm^{-2} was applied to HL-60, K562, U937, and M1/2 leukemia cell line cultures. Lower acoustic amplitudes of 22.4 W cm^{-2} spatial-peak temporal-average intensity were used as a control. Although it is well known that high-intensity ultrasound causes inertial cavitation effects, the authors were able to demonstrate the induction of programmed cell death, i.e., apoptosis, which holds promise for cancer therapy. Interestingly, the effects were similar to those produced by gamma radiation.

Cultured vascular endothelial cells were subjected to eight repetitions of sonication for 1 min each experiment with unspecified high-frequency ultrasound at 2.5 W cm^{-2} in the presence of plasmid DNA with and without an ultrasound contrast agent present [83]. In addition, in-vivo sonication under similar conditions was performed for 2 min on a damaged rat carotid artery in the presence of DNA. In both cases, transfection of DNA into cells was achieved with higher efficiency under sonication, and even more so in the presence of the ultrasound contrast agent. This paper is generally considered as fundamental proof that cells themselves may respond to ultrasound at acoustic conditions below the inertial cavitation threshold.

The cytotoxic effect of low-energy ultrasound at 7 mW mL^{-1} acoustical power was evaluated for various exposure times ranging from 30 min to 5 h at a frequency of 1.8 MHz and on/off cycle of 5.5 ms/3 ms [84]. Normal mononuclear cells, primary leukaemic cells and four leukaemic cell lines were studied. The authors demonstrated that necrosis is significantly diminished while apoptosis is stimulated in leukaemic cells. They also demonstrated that ultrasound exposure is linked to oxidative stress, and that active oxygen scavengers reduce the effect of ultrasound on apoptosis, suggesting a sonochemical mechanism.

A bacterium *E. coli* and a yeast species *S. cerevisiae* were studied under ultrasound sonication with a view to producing cell lysis as a first step in various diagnostic processes [85]. Sonication was achieved using a spherically focussed 1-MHz ultrasound beam in a specially designed sonication chamber. Treatment was at 5.2 W cm^{-2} for 30 s, which resulted in greater than 99% loss in viability of both cell types. However, the yeasts demonstrated a relative resistance to disruption and further chemical techniques were needed to liberate cell contents.

The transfer of DNA into cells has clinical, bio-industrial and environmental applications [86]. This study investigated the use of 40-kHz ultrasound to achieve DNA transfer into a variety of bacterial species. In the centre of the experimental bath used, the estimated intensity was 240 mW cm^{-2} . The optimal duration of sonication was chosen to be 10 s, as an optimal compromise between the competing requirements of efficiency of DNA transfer and minimising ultrasound-induced loss of cell viability. Sonication is the putative mechanism for ultrasound-based DNA transfer and it proved substantially more efficient than the commonly used methods of electroporation and conjugation.

The combined effects of low-intensity pulsed ultrasound and doxorubicin (DOX) on cell killing and apoptosis induction of human myelomonocytic lymphoma U937 cells was investigated in vitro [87].

The experiments were conducted in four groups, including an ultrasound-treated group and a combined ultrasound and DOX-treated group. Cells were exposed to 5 μM DOX for 30 min and sonicated 60 s by 1-MHz pulsed ultrasound with a 100-Hz pulse-repetition frequency and a 10% duty cycle. The acoustic intensities varied between 0.2 and 0.5 W cm^{-2} . No cell killing or induction of apoptosis was observed at 0.2 W cm^{-2} . However, cell killing, induction of apoptosis, and hydroxyl radical formation were detected at intensities equal to and greater than 0.3 W cm^{-2} . More radicals were produced in the combined ultrasound and DOX group than with ultrasound alone. Yoshida et al. hypothesised that DOX treatment weakens cell membranes, so that sonoporation is more successful.

Sonication with 40-kHz ultrasound was shown to inhibit growth of Gram-negative bacteria with species such as *E. coli* showing sufficient sensitivity that they were eradicated in as little as 5 min [88]. Gram-positive bacteria, however, were resistant to sonication. This study shows that inhibition of bacteria by sonication is dependent on a number of factors including species, temperature, and duration of sonication. The results have implications for the management of bacterial infections of prosthetic implants which represent an important cause of morbidity and implant failure.

In a study on the ultrasound-induced inactivation of Gram-negative and Gram-positive bacteria in secondary treated municipal waste water [89], various bacterial species were subjected to 24 kHz of 1500 W L^{-1} , corresponding to 5400 kJ L^{-1} specific nominal energy, for a duration of 60 min in the presence and absence of titanium dioxide particles. Gram-negative bacteria proved to be highly susceptible to inactivation by sonication using this regime, showing a response of greater than 99%. Gram-positive bacteria showed substantially lower inactivation rates. Adding titanium dioxide enhanced the response of both Gram-negative and Gram-positive bacteria to the destructive effect of sonication. However, this enhancement was far more modest in the case of Gram-positive bacteria.

To investigate the effect of diagnostic ultrasound on blue-green algae eradication in a laboratory setup [90], three undamped single-element ultrasound transducers were used, with centre frequencies of 200-kHz, 1-MHz, and a 2.2-MHz, respectively. The transducers were subjected to 16-Vpp square pulses at an 11.8-kHz pulse-repetition rate. Low acoustic amplitudes were used in order to comply with an MI below 0.3. The peak-negative acoustic pressures were 40 kPa for the 1-MHz transducer and 68 kPa for the 2.2-MHz transducer, respectively. The blue-green algae used were of the *Anabaena sphaerica* species. Blue-green algae were forced within minutes to sink at the ultrasonic frequencies studied, thus supporting the hypothesis that heterocysts release gaseous nitrogen during sonication. A similar study had been done on a different cyanobacteria species, *Microcystis aeruginosa* [91]. Beakers were sonicated during 5 min at 25 kHz at 0.32 W mL^{-1} , which inhibited growth. Fourteen days after sonication, the cell concentration was only 14.1% of the control sample.

To investigate the effect of low-intensity ultrasound on DNA [92], 1.0-MHz ultrasound with 100-Hz fixed pulse-repetition frequency and 10% duty cycle was generated during 1 min in culture dishes containing four different leukaemia cell lines, U937, Molt-4, Jurkat, and HL-60, at intensities of 0.1, 0.2, 0.3, and 0.4 W cm^{-2} , corresponding to acoustic pressure amplitudes of 0.061, 0.105, 0.132, and 0.144 MPa, respectively. Only at the two highest intensities were DNA double-strand breaks with all cell lines observed. This damaging effect was attributed to mechanical stress.

A modified experimental setup was used to carry out ultrasound-assisted gene transfection [93]. Sonication was carried out using 1.0-MHz ultrasound at an intensity of 0.3 W cm^{-1} and a 50% duty cycle with a 5-Hz pulse-repetition frequency. Dishes containing HeLa cells in the presence of free plasmid DNA (pDNA) were sonicated immediately after preparation for periods of 30 s or 15 min. The results showed that ultrasound enhances the intracellular trafficking of previously internalised genes when longer sonication periods are applied.

There is a need to have techniques to disrupt (lyse) cells in order to release their contents for the purpose of drug development and other biological research [94]. Detergent-based disruption frequently has unfavourable effects on cells. Ly et al. developed an ultrasonic method to affect this disruption. Medical Research Council cell strain 5 (MRC-5) cells infected with an attenuated Varicella-Zoster virus

were subjected to ultrasound of intensities from $0.1\text{--}10\text{ W cm}^{-2}$ and at duty cycles of 0.1–20%. Cell lysis was achieved.

Most experimental studies in this section resulted in lysis. If we regard sonoporation as unsuccessful lysis, we might explain why both phenomena are observed in the same acoustic regimes. Apoptosis is less often observed. This phenomenon is associated with high MI and the formation of free radicals.

The experimental studies with bacteria were performed under unclear conditions. It would be interesting to compare acoustic lysis thresholds for mixtures of desirable and undesirable cells.

2.3. Translation

This section gives an overview of cellular acoustics studies that resulted in the translation of cells. The studies have been treated in chronological order.

To investigate the effects of ultrasound on blood platelets, platelet-rich plasma and washed platelets were treated with 22-kHz ultrasound at intensities ranging from 1 to 8.8 W cm^{-2} over multiple seconds [95]. Sonication of a calcium-containing preparation resulted in intensity- and time-dependent platelet aggregation. This effect, however, was absent in a calcium-free medium. Both the calcium-containing and calcium-free preparations showed a substantial increase in intracellular calcium in response to sonication.

Zourob et al. addressed the need to reliably and sensitively detect bacteria without the time-consuming step of culture [96]. A sonication and detection chamber was constructed. The chamber included an ultrasound-producing piezoelectric transducer and a specially designed optical metal-clad leaky waveguide (MCLW) with immobilised antibodies on the surface which, using optical techniques, served as the bacterial detector. This MCLW detector was created by depositing the cladding on a 1-mm glass slide that served as a half-wavelength ultrasound reflector, resulting in ultrasound standing waves, with a node forming at the detector-water interface at a frequency of 3 MHz. This caused bacterial spores to collect at the detector during sonication through radiation forces. Stepping the ultrasound in 20-kHz increments from 2 to 4 MHz, it was found that 2.94 MHz was a suitable operating frequency as it represented the maximum voltage difference between the water-filled and empty chamber and was assumed to represent a resonance in the water. As the chamber was a quarter wavelength long, only a single node could form. Sonication for 3 min caused the bacterial spores to move efficiently towards the detector and form regular patterns at the detector surface. These patterns varied in their appearance with ultrasound frequency changes as small as 150 kHz. Increasing the applied peak-to-peak voltage, which is proportional to sound pressure, resulted in increased bacterial spore capture at the interface up to a maximum of 4 V, after which the bacterial spore capture diminished due to the formation of aggregates.

In a similar experimental setup as the one used by Mizrahi et al. [97], endothelial cells were subjected to 1-MHz ultrasound with acoustic pressure amplitudes between 50 kPa and 300 kPa and a duration of 5 min at a 20% duty cycle [26]. Endothelial detachment was observed, followed by the geometric reorganisation of the cells according to a periodic pattern, corresponding to nodes or antinodes of the sound field. In addition, sonication caused increased clustering of $\alpha V\beta 3$ integrin, a transmembrane protein. However, sonication did not change the amount of β -actin monomers, which are involved in reshaping of the cell.

The accumulation of cells in the nodes or antinodes of a sound field was also described in a study to separate bacterial *E. coli* cells and yeast cells, sonicated at 1 MHz and 3 MHz [98].

Following an early review on acoustic manipulation [15], several studies were published on devices that use sound to force cells to translate. Optical observations of the clustering behaviour of living cells and several other particles were done in a standing sound field at 1 MHz or 3 MHz continuous-wave ultrasound with peak-to-peak amplitudes between 1 V and 10 V, generated inside a ring transducer [99]. Upon sonication, blood cells were observed to become trapped in the nodes of the ultrasound field owing to primary radiation forces. It was found that red blood cells and hydrophobic particles translate like a particle trapped inside a thin gas shell. In fact, the sonophore

model mentioned treats biological cells in a similar way [58]. Cells have also proven to be responsive to acoustic radiation forces at a frequency much higher than used in the former study [99], making single cell-type-specific cell sorting feasible [100,101]. The latter studies used a device operating with standing waves of 19.4 MHz [100,101]. A similar device for the identification, separation and cell-type specific manipulation of not single but multiple biological cells was also designed and built [102]. Cultured cells in a Petri dish were sonicated at 7-MHz continuous-wave ultrasound for 30 s. After sonication, Chinese hamster ovary (CHO) cells were seen to have formed clusters of packed cells whilst human embryonic kidney (HEK) cells did not show cluster formation at all. The experiments were done with separate CHO and HEK cell cultures, and a mixture thereof. In a mixture of both CHO and HEK cell cultures, only the cells of one type cluster. It was concluded that different cell types may behave differently at the same ultrasound frequency.

Most experimental studies resulting in translation were carried out in standing wave fields. Therefore, cell aggregation is the most-observed translation phenomenon. It is interesting to trace cell translation speed as a function of cell bulk modulus. If subtle cell stiffness differences result in a significant speed difference, individual cancer cells or parasite-infested cells might be traced acoustically.

2.4. Proliferation

This section gives an overview of cellular acoustics studies that resulted in changed proliferation of cells. The studies have been treated in chronological order.

Sonication at intensities of up to 2 W cm^{-2} at 70 kHz of three bacterial species, *viz.*, *S. epidermidis*, *E. coli*, and *P. aeruginosa*, demonstrated increased biofilm and planktonic growth compared to the absence of sonication [103]. Greater intensities resulted in inhibition of bacterial adhesion to surfaces. Continuous-wave ultrasound was administered in these experiments except in the case of *P. aeruginosa*, where a 1:5 duty cycle was used and delivered in 100-ms pulses with pulse-repetition every 500 ms for 48 h. The authors propose an enhanced mass transport phenomenon as the basis for the increased bacterial growth.

Cultured bovine aortic endothelial cells were subjected to sonication for 15 and 30 min at intensities 1.2 W cm^{-2} at frequencies of 0.5, 1.0, 3.5, and 5.0 MHz in both pulsed-wave (50% duty cycle) and continuous-wave modes [104]. Increased cell proliferation was evident in the ultrasound-treated cells compared to the non-sonicated controls, with continuous-wave mode having a greater effect on proliferation than pulsed mode. Transmit frequency did not have a statistically significant effect in the range studied, and the proliferation effect became more prominent with elapsed time after sonication up to the 72 h studied. Sonication also produced transient partial disassembly of structures such as actin stress fibres and microtubules. This effect was resolved within a few hours after sonication. This study is thought to have implications for ultrasound-based promotion of wound healing.

Whilst the 2007 study of Hultström et al. describes experiments on acoustic cell trapping in a microfluidic channel, it was found that 30–75 min of sonication with a 3-MHz standing wave field with a pressure amplitude of 0.85 MPa was beneficial to the proliferation of CV-1 in origin simian line 7 (COS-7) cells [105].

The observation that increased proliferation is frequency-independent hints at a temperature-related effect. This is supported by the fact that continuous wave augments proliferation. Null experiments are required at slightly incremented temperatures to determine, whether temperature or vibration is of influence on cell proliferation.

2.5. Internal Changes

This section gives an overview of cellular acoustics studies that resulted in changes inside the cells. The studies have been treated in chronological order.

Rabbit corneas were exposed *in vivo* to continuous-wave ultrasound at a frequency of 880 kHz and with intensities ranging from 0.19 to 0.56 W cm^{-2} for 5 min [106]. These intensities correspond

to ultrasound pressures of 0.08 to 0.13 MPa and mechanical indices of 0.08 to 0.14. The increasing intensities of sonication caused sodium fluorescein, a hydrophilic dye introduced onto the corneal surface, to appear in the fluid of the anterior eye at higher concentrations than in non-sonicated eyes, with concentration increases over non-sonicated eyes ranging from more than double, to more than 10-fold at the highest intensities. Microscopic and macroscopic examination of the corneas after sonication revealed structural changes in the surface layer of cells including pits, but not in the deeper layers. These changes reversed after approximately 90 min.

Or et al. proposed that relative oscillatory displacements between intracellular structures may explain the effects of low to medium intensity ultrasound on cells and tissues [107]. Such effects include modulation of action potentials in excitable tissues, modulation of angiogenesis, changes in membrane permeability and modulation of molecular expression. The authors constructed a linear model for a spherical object which is intended to approximate an intracellular structure such as a nucleus embedded within a homogeneous viscoelastic medium. Maximal amplitude vibrations are found in the sub-MHz range with the specific frequencies at which maximum oscillations occur being consistent with resonance phenomena. The authors suggested that the very small intracellular strain associated with these conditions, through a cyclic fatigue-like mechanism may be responsible for the biological effects.

As a first attempt to explain sub-cavitation threshold cellular acoustics [58], studies in which fish epidermis cells had been subjected to both cavitation-inducing 1-MHz, and non-cavitation inducing 3-MHz continuous-wave ultrasound [108] were re-examined. It was shown that there is a graded range of biological effects which includes behaviours that do not involve cavitation. The authors were also able to demonstrate ultrasound-induced changes to cellular organelles. The cellular response to ultrasound was attributed to the formation of gas bubbles inside the bilayer cell membrane, the so-called sonophore hypothesis [58].

In a follow-up study by the same group [97], real-time in-vitro microscopic studies were performed on cells subjected to uniform pulsed 1-MHz ultrasound with a 20% duty cycle and intensities of 1 W cm^{-2} and 2 W cm^{-2} , corresponding to hydrophone-measured acoustic pressure amplitudes of 170 kPa and 290 kPa, respectively. Substantial cytoskeletal changes and remodelling were evident at higher intensities corresponding to remarkably small strain values.

In a very recent study on the effect of low-intensity ultrasound and mesenchymal-epithelial (MET) signaling on cellular motility and morphology [109], continuous-wave low-intensity ultrasound of 200-kPa pressure amplitude at 960 kHz was applied to cells from a Madin–Darby canine kidney (MDCK) cell line. The putative basis for the effects on the MDCK cell membrane is the bilayer sonophore model whereby intramembrane cavitation occurs at moderate acoustic amplitudes. The authors have demonstrated that their setup results in modulation of the so-called MET tyrosine kinase signalling pathway which in turn modifies cell morphology and diminishes critical cancer cell behaviour such as motility. This may form the basis of novel cancer therapies.

The experimental studies in this section were performed at $MI < 0.3$. Low-amplitude sonication causes subtle intracellular effects. Follow-up research must validate the sonophore hypothesis or provide an alternative explanation for the phenomena observed.

3. Conclusions

This article reviews those effects of ultrasound on living cells that do not include inertial cavitation, cellular effects due to the introduction of bubbles, and non-destructive structural evaluation through ultrasonic biomicroscopy.

The main effects witnessed in the publications reviewed in this article have been summarised in Table 1.

Table 1. Overview of publications on cellular ultrasonics in chronological order.

Cell Type	Frequency	Amplitude	Main Effect	Ref.
Newt notochord	1 MHz	8–15 W cm ⁻²	Disruption	[66]
Blood	2.25 MHz	30 mW	Chromosomal damage	[67]
Frog muscle	85 kHz	1–5 μm	Structure disruption	[68]
<i>Elodea</i>	0.45–10 MHz	75–180 mW cm ⁻²	Cell death	[71,72]
Platelets	1–10 MHz	0.5–76 kPa	Streaming	[75]
Platelets	1 MHz	0.2, 0.6 W cm ⁻²	Disruption	[76]
<i>Erythrocytes</i>	1 MHz	0–5 W cm ⁻²	Lysis	[77]
<i>Erythrocytes</i>	24 kHz	100 kPa–1 MPa	Permeation	[78]
HL-60	255 kHz	0.4 W cm ⁻²	Membrane changes	[79]
<i>B. subtilis</i>	22–67 kHz	20–60 W	Lysis	[80]
<i>B. subtilis</i>	40 kHz	25–38 μm	Lysis	[81]
Leukaemic	750 kHz	22.4–103.7 W cm ⁻²	Apoptosis	[82]
Platelets	22 kHz	1–8.8 W cm ⁻²	Aggregation	[95]
Endothelial		2.5 W cm ⁻²	Permeation	[83]
Leukaemic	1.8 MHz	7 mW mL ⁻¹	Apoptosis	[84]
<i>E. coli</i>	1 MHz	5.2 W cm ⁻²	Eradication	[85]
<i>S. cerevisiae</i>	1 MHz	5.2 W cm ⁻²	Eradication	[85]
<i>S. epidermidis</i>	75 kHz	2 W cm ⁻²	Proliferation	[103]
<i>E. coli</i>	75 kHz	2 W cm ⁻²	Proliferation	[103]
<i>P. aeruginosa</i>	75 kHz	2 W cm ⁻²	Proliferation	[103]
Cornea	880 kHz	0.19–0.56 W cm ⁻²	Structural changes	[106]
Endothelial	0.5–5 MHz	1.2 W cm ⁻²	Proliferation	[104]
Bacterial spores	2–4 MHz		Translation	[96]
COS-7	3 MHz	0.85 MPa	Proliferation	[105]
Bacteria	40 kHz	240 mW cm ⁻²	Permeation	[86]
U937	1 MHz	0.3–0.5 W cm ⁻²	Apoptosis	[87]
Bacteria	40 kHz		Eradication	[88]
Bacteria	24 kHz	1500 W L ⁻¹	Eradication	[89]
<i>Anabaena sphaerica</i>	200 kHz–2.2 MHz	40–68 kPa	Disruption	[90]
<i>Microcystis aeruginosa</i>	25 kHz	0.32 W mL ⁻¹	Proliferation	[91]
Fish epidermis	3 MHz	2.2 W cm ⁻²	Organelle changes	[58,108]
HASM	1 MHz	1 W cm ⁻² , 2 W cm ⁻²	Cytoskeletal changes	[97]
Endothelial	1 MHz	50–300 kPa	Translation	[26]
Leukaemic	1 MHz	0.3–0.4 W cm ⁻²	DNA breakage	[92]
HeLa	1 MHz	0.3 W cm ⁻²	Permeation	[93]
MRC-5		0.1–10 W cm ⁻²	Lysis	[94]
<i>Erythrocytes</i>	1 MHz, 3 MHz	1–10 V	Translation	[99]
MCF-7, leukocytes	19.4 MHz	2 W cm ⁻²	Separation	[100,101]
CHO, HEK	7 MHz		Separation	[102]
MDCK	960 kHz	200 kPa	Morphology changes	[109]

Transient and permanent cell disruption dominate Table 1 with 22 out of 40 publications. However, these studies are included because the underlying mechanism for these effects in most cases do not appear to be due to inertial cavitation or to result directly from the introduction of bubbles, or because the nature of the effect is uncertain due to a paucity of information about the acoustic intensities. The remaining 18 papers describe more subtle effects at moderate intensities, such as translation (seven publications), internal changes (five publications), and proliferation (six publications).

Living cells under the influence of ultrasound may experience proliferation, translation, apoptosis, lysis, transient membrane permeation, and oscillation. Cytoskeletal and internal changes have been reported.

Future research will concentrate on finding lysis thresholds of different cell types, with the purpose of eradicating unwanted cells whilst leaving healthy, wanted, cells unharmed. Detectable differences in translation speeds of individual cells might be future acoustic identifiers of cancer or malaria. Cell proliferation is augmented by sonication at any frequency, which means that mechanical effects

are not a probable cause of the proliferation observed. Consequently, combined heating and vibrating of wounded tissue might be investigated as a means for accelerated healing. Moreover, the formation of sonophores needs to be validated or alternative explanations for intracellular changes in low-MI ultrasound fields must be explored. Ultrasound itself can manipulate and damage cells at low acoustic amplitudes. It is therefore worthwhile to develop truly noninvasive ultrasound-based therapeutic methods. The ultimate goal of cellular acoustics is the detection, quantification, manipulation and eradication of individual cells.

Author Contributions: N.A., C.S., J.P., and M.N. contributed; D.M.R. and M.P. wrote the paper.

Funding: This research received no external funding.

Conflicts of Interest: The authors declare no conflict of interest.

Abbreviations

The following abbreviations are used in this manuscript:

CHO	Chinese hamster ovary;
COS-7	CV-1 in origin simian line 7
DNA	deoxyribonucleic acid
DOX	doxorubicin
HASM	human airway smooth muscle
HEK	human embryonic kidney
HeLa	Henrietta Lacks
HIFU	high-intensity focussed ultrasound
HL	human leukaemia
MCF-7	Michigan Cancer Foundation cell line 7
MCLW	metal-clad leaky waveguide
MDCK	Madin–Darby canine kidney
MET	mesenchymal-epithelial
MI	mechanical index
MRC-5	Medical Research Council cell strain 5
PCR	polymerase chain reaction
pDNA	plasmid DNA
PNP	peak-negative pressure
PPP	peak-positive pressure
PRF	pulse-repetition frequency
PRT	pulse-repetition time
P2P	peak-to-peak pressure

References

1. ter Haar, G.R. HIFU tissue ablation: Concept and devices. In *Therapeutic Ultrasound*; Escoffre, J.M., Bouakaz, A., Eds.; Springer: Berlin, Germany, 2016; Volume 880, pp. 3–20. [[CrossRef](#)]
2. Eisenmenger, W. The mechanisms of stone fragmentation in ESWL. *Ultrasound Med. Biol.* **2001**, *27*, 683–693. [[CrossRef](#)]
3. Dimceviski, G.; Kotopoulis, S.; Bjånes, T.; Hoem, D.; Schjøtt, J.; Gjertsen, B.T.; Biermann, M.; Molven, A.; Sorbye, H.; McCormack, E.; et al. A human clinical trial using ultrasound and microbubbles to enhance gemcitabine treatment of inoperable pancreatic cancer. *J. Control. Release* **2016**, *243*, 172–181. [[CrossRef](#)] [[PubMed](#)]
4. Kaneko, Y.; Maruyama, T.; Takegami, K.; Watanabe, T.; Mitsui, H.; Hanajiri, K.; Nagawa, H.; Matsumoto, Y. Use of a microbubble agent to increase the effects of high intensity focused ultrasound on liver tissue. *Eur. Radiol.* **2005**, *15*, 1415–1420. [[CrossRef](#)] [[PubMed](#)]
5. van Wamel, A.; Sontum, P.C.; Healey, A.J.; Kvåle, S.; Bush, N.; Bamber, J.; de Lange Davies, C. Acoustic cluster therapy (ACT) enhances the therapeutic efficacy of paclitaxel and Abraxane for treatment of human prostate adenocarcinoma in mice. *J. Control. Release* **2016**, *236*, 15–21. [[CrossRef](#)] [[PubMed](#)]

6. van der Windt, D.A.; van der Heijden, G.J.; van den Berg, S.G.; ter Riet, G.; de Winter, A.F.; Bouter, L.M. Ultrasound therapy for musculoskeletal disorders: A systematic review. *Pain* **1999**, *81*, 257–271. [[CrossRef](#)]
7. Desmeules, F.; Boudreault, J.; Roy, J.S.; Dionne, C.; Frémont, P.; MacDermid, J.C. The efficacy of therapeutic ultrasound for rotator cuff tendinopathy: A systematic review and meta-analysis. *Phys. Ther. Sport* **2015**, *16*, 276–284. [[CrossRef](#)] [[PubMed](#)]
8. Harle, J.; Salih, V.; Mayia, F.; Knowles, J.C.; Olsen, I. Effects of ultrasound on the growth and function of bone and periodontal ligament cells in vitro. *Ultrasound Med. Biol.* **2001**, *27*, 579–586. [[CrossRef](#)]
9. Lim, K.; Kim, J.; Seonwoo, H.; Park, S.H.; Choung, P.H.; Chung, J.H. In vitro effects of low-intensity pulsed ultrasound stimulation on the osteogenic differentiation of human alveolar bone-derived mesenchymal stem cells for tooth tissue engineering. *BioMed Res. Int.* **2013**, *2013*, 269724. [[CrossRef](#)] [[PubMed](#)]
10. Nakao, J.; Fujii, Y.; Kusuyama, J.; Bandow, K.; Kakimoto, K.; Ohnishi, T.; Matsuguchi, T. Low-intensity pulsed ultrasound (LIPUS) inhibits LPS-induced inflammatory responses of osteoblasts through TLR4–MyD88 dissociation. *Bone* **2014**, *58*, 17–25. [[CrossRef](#)] [[PubMed](#)]
11. Schumann, D.; Kujat, R.; Zellner, J.; Angele, M.K.; Nerlich, M.; Mayr, E.; Angele, P. Treatment of human mesenchymal stem cells with pulsed low intensity ultrasound enhances the chondrogenic phenotype in vitro. *Biorheology* **2006**, *43*, 431–443. [[PubMed](#)]
12. Dalla-Bona, D.A.; Tanaka, E.; Inubushi, T.; Oka, H.; Ohta, A.; Okada, H.; Miyauchi, M.; Takata, T.; Tanne, K. Cementoblast response to low- and high-intensity ultrasound. *Arch. Oral Biol.* **2008**, *53*, 318–323. [[CrossRef](#)] [[PubMed](#)]
13. Takeuchi, R.; Ryo, A.; Komitsu, N.; Mikuni-Takagaki, Y.; Fukui, A.; Takagi, Y.; Shiraishi, T.; Morishita, S.; Yamazaki, Y.; Kumagai, K.; et al. Low-intensity pulsed ultrasound activates the phosphatidylinositol 3 kinase/Akt pathway and stimulates the growth of chondrocytes in three-dimensional cultures: A basic science study. *Arthritis. Res. Ther.* **2008**, *10*, R77. [[CrossRef](#)] [[PubMed](#)]
14. Bazou, D.; Maimon, N.; Munn, L.L.; Gonzalez, I. Effects of low intensity continuous ultrasound (LICU) on mouse pancreatic tumor explants. *Appl. Sci.* **2017**, *7*, 1275. [[CrossRef](#)]
15. Wiklund, M. Acoustofluidics 12: Biocompatibility and cell viability in microfluidic acoustic resonators. *Lab Chip* **2012**, *12*, 2018–2028. [[CrossRef](#)] [[PubMed](#)]
16. O'Brien, W.D., Jr. Ultrasound–biophysics mechanisms. *Prog. Biophys. Mol. Biol.* **2007**, *93*, 212–255. [[CrossRef](#)] [[PubMed](#)]
17. Wu, J.; Nyborg, W.L. Ultrasound, cavitation bubbles and their interaction with cells. *Adv. Drug Deliv. Rev.* **2008**, *60*, 1103–1116. [[CrossRef](#)] [[PubMed](#)]
18. Shankar, H.; Pagel, P.S. Potential adverse ultrasound-related biological effects: a critical review. *Anesthesiology* **2011**, *115*, 1109–1124. [[CrossRef](#)] [[PubMed](#)]
19. Izadifar, Z.; Babyn, P.; Chapman, D. Mechanical and biological effects of ultrasound: A review of present knowledge. *Ultrasound Med. Biol.* **2017**, *43*, 1085–1104. [[CrossRef](#)] [[PubMed](#)]
20. Tortora, G.J.; Derrickson, B.H. *Principles of Anatomy and Physiology*, 13th ed.; Wiley: Philadelphia, PA, USA, 2008.
21. Yang, T.; Bragheri, F.; Nava, G.; Chiodi, I.; Mondello, C.; Osellame, R.; Berg-Sørensen, K.; Cristiani, I.; Minzioni, P. A comprehensive strategy for the analysis of acoustic compressibility and optical deformability on single cells. *Sci. Rep.* **2016**, *6*, 23946. [[CrossRef](#)] [[PubMed](#)]
22. Tomlinson, M.J.; Tomlinson, S.; Yang, X.B.; Kirkham, J. Cell separation: terminology and practical considerations. *J. Tissue Eng.* **2013**, *4*, 2041–7314. [[CrossRef](#)] [[PubMed](#)]
23. Postema, M. *Fundamentals of Medical Ultrasonics*; Spon: London, UK, 2011; ISBN 978-1135-179-36-6.
24. Nowicki, A. *Ultradźwięki w medycynie: wprowadzenie do współczesnej ultrasonografii*; Instytut Podstawowych Problemów Techniki, Polska Akademia Nauk: Warszawa, Poland, 2010.
25. Postema, M.; Kotopoulis, S.; Jenderka, K.V. Basic physical principles of medical ultrasound. In *EFSUMB Course Book on Ultrasound*; Dietrich, C.F., Ed.; EFSUMB: London, UK, 2012; pp. 9–37.
26. Geffen, C.; Kimmel, E. The effect of low intensity ultrasound on adhesion molecules, actin monomers and membrane permeability in endothelial cells. In *Micro-Acoustics in Marine and Medical Research*; Kotopoulis, S., Delalande, A., Godø, O.R., Postema, M., Eds.; Institutt for fysikk og teknologi, Universitetet i Bergen: Bergen, Norway, 2012; pp. 131–170.
27. Dehoux, T.; Abi Ghanem, M.; Zouani, O.F.; Rampnoux, J.M.; Guillet, Y.; Dilhaire, S.; Durrieu, M.C.; Audoin, B. All-optical broadband ultrasonography of single cells. *Sci. Rep.* **2015**, *5*, 8650. [[CrossRef](#)] [[PubMed](#)]

28. Blase, C.; Bereiter-Hahn, J. Ultrasonic characterization of biological cells. In *Ultrasonic and Electromagnetic NDE for Structure and Material Characterization: Engineering and Biomedical Applications*; Kundu, T., Ed.; CRC: Boca Raton, FL, USA, 2012; pp. 689–722.
29. Silberrad, O. Propeller erosion. *Engineering* **1912**, *33*, 33–35.
30. Brennen, C.E. *Cavitation and Bubble Dynamics*; Oxford: New York, NY, USA, 1995.
31. Young, F.R. *Cavitation*; McGraw-Hill: New York, NY, USA, 1989.
32. Kondo, T.; Fukushima, Y.; Kon, H.; Riesz, P. Effect of shear stress and free radicals induced by ultrasound on erythrocytes. *Arch. Biochem. Biophys.* **1989**, *269*, 381–389. [[CrossRef](#)]
33. Riesz, P.; Kondo, T. Free radical formation induced by ultrasound and its biological implications. *Free Radic. Biol. Med.* **1992**, *13*, 247–270. [[CrossRef](#)]
34. Carstensen, E.L.; Kelly, P.; Church, C.C.; Brayman, A.A.; Child, S.Z.; Raeman, C.H.; Schery, L. Lysis of erythrocytes by exposure to CW ultrasound. *Ultrasound Med. Biol.* **1993**, *19*, 147–165. [[CrossRef](#)]
35. Dalecki, D. Mechanical bioeffects of ultrasound. *Cancer Res.* **2004**, *6*, 229–248. [[CrossRef](#)] [[PubMed](#)]
36. Rosenthal, I.; Sostaric, J.Z.; Riesz, P. Sonodynamic therapy—a review of the synergistic effects of drugs and ultrasound. *Ultrasoun. Sonochem.* **2004**, *11*, 349–363. [[CrossRef](#)] [[PubMed](#)]
37. Harvey, E.N.; Loomis, A.L. High frequency sound waves of small intensity and their biological effects. *Nature* **1928**, *121*, 622–624. [[CrossRef](#)]
38. Harvey, E.N.; Harvey, E.B.; Loomis, A.L. Further observations on the effect of high frequency sound waves on living matter. *Biol. Bull.* **1928**, *55*, 459–469. [[CrossRef](#)]
39. British Medical Ultrasound Society. Guidelines for the Safe Use of Diagnostic Ultrasound Equipment. *SAGE J.* **2000**, *18*, 52–59.
40. ter Haar, G. Safety and bio-effects of ultrasound contrast agents. *Med. Biol. Eng. Comput.* **2009**, *47*, 893–900. [[CrossRef](#)] [[PubMed](#)]
41. Postema, M.; Gilja, O.H. Contrast-enhanced and targeted ultrasound. *World J. Gastroenterol.* **2011**, *17*, 28–41. [[CrossRef](#)] [[PubMed](#)]
42. Voigt, J.U. Ultrasound molecular imaging. *Methods* **2009**, *48*, 92–97. [[CrossRef](#)] [[PubMed](#)]
43. Postema, M.; van Wamel, A.; Lancée, C.T.; de Jong, N. Ultrasound-induced encapsulated microbubble phenomena. *Ultrasound Med. Biol.* **2004**, *30*, 827–840. [[CrossRef](#)] [[PubMed](#)]
44. Heppner, P.; Lindner, J.R. Contrast ultrasound assessment of angiogenesis by perfusion and molecular imaging. *Expert Rev. Mol. Diagn.* **2005**, *5*, 447–455. [[CrossRef](#)] [[PubMed](#)]
45. Prentice, P.; Cuschieri, A.; Dholakia, K.; Prausnitz, M.; Campbell, P. Membrane disruption by optically controlled microbubble cavitation. *Nat. Phys.* **2005**, *1*, 107–110. [[CrossRef](#)]
46. Sundaram, J.; Mellein, B.R.; Mitragotri, S. An experimental and theoretical analysis of ultrasound-induced permeabilization of cell membranes. *Biophys. J.* **2003**, *84*, 3087–3101. [[CrossRef](#)]
47. Kudo, N.; Okada, K.; Yamamoto, K. Sonoporation by single-shot pulsed ultrasound with microbubbles adjacent to cells. *Biophys. J.* **2009**, *96*, 4866–4876. [[CrossRef](#)] [[PubMed](#)]
48. Keyhani, K.; Guzmán, H.R.; Parsons, A.; Lewis, T.N.; Prausnitz, M.R. Intracellular drug delivery using low-frequency ultrasound: Quantification of molecular uptake and cell viability. *Pharm. Res.* **2001**, *18*, 1514–1520. [[CrossRef](#)] [[PubMed](#)]
49. Postema, M.; Gilja, O.H. Ultrasound-directed drug delivery. *Curr. Pharm. Biotechnol.* **2007**, *8*, 355–361. [[CrossRef](#)] [[PubMed](#)]
50. Lee, N.G.; Berry, J.L.; Lee, T.C.; Wang, A.T.; Honowitz, S.; Murphree, A.L.; Varshney, N.; Hinton, D.R.; Fawzi, A.A. Sonoporation enhances chemotherapeutic efficacy in retinoblastoma cells in vitro. *Investig. Ophthalmol. Vis. Sci.* **2011**, *52*, 3868–3873. [[CrossRef](#)] [[PubMed](#)]
51. Delalande, A.; Postema, M.; Mignet, N.; Midoux, P.; Pichon, C. Ultrasound and microbubble-assisted gene delivery: recent advances and ongoing challenges. *Therap. Deliv.* **2012**, *3*, 1199–1215. [[CrossRef](#)]
52. Kaufman, G.E.; Miller, M.W.; Griffiths, T.D.; Ciaravino, V.; Carstensen, E.L. Lysis and viability of cultured mammalian cells exposed to 1 MHz ultrasound. *Ultrasound Med. Biol.* **1977**, *3*, 21–25. [[CrossRef](#)]
53. Brayman, A.A.; Coppage, M.L.; Vaidya, S.; Miller, M.W. Transient poration and cell surface receptor removal from human lymphocytes in vitro by 1 MHz ultrasound. *Ultrasound Med. Biol.* **1999**, *25*, 999–1008. [[CrossRef](#)]
54. Firestein, F.; Rozenszajn, L.A.; Shemesh-Darvish, L.; Elimelech, R.; Radnay, J.; Rosenschein, U. Induction of apoptosis by ultrasound application in human malignant lymphoid cells: role of mitochondria-caspase pathway activation. *Ann. N. Y. Acad. Sci.* **2003**, *1010*, 163–166. [[CrossRef](#)] [[PubMed](#)]

55. Duvshani-Eshet, M.; Machluf, M. Therapeutic ultrasound optimization for gene delivery: A key factor achieving nuclear DNA localization. *J. Control. Release* **2005**, *108*, 513–528. [[CrossRef](#)] [[PubMed](#)]
56. Delalande, A.; Kotopoulos, S.; Rovers, T.; Pichon, C.; Postema, M. Sonoporation at a low mechanical index. *Bubble Sci. Eng. Technol.* **2011**, *3*, 3–12. [[CrossRef](#)]
57. Johansen, K.; Kimmel, E.; Postema, M. Theory of red blood cell oscillations in an ultrasound field. *Arch. Acoust.* **2017**, *42*, 121–126. [[CrossRef](#)]
58. Krasovitski, B.; Frenkel, V.; Shoham, S.; Kimmel, E. Intramembrane cavitation as a unifying mechanism for ultrasound-induced bioeffects. *Proc. Natl Acad. Sci. USA* **2011**, *108*, 3258–3263. [[CrossRef](#)] [[PubMed](#)]
59. Johansen, K.; Postema, M. Lagrangian formalism for computing oscillations of spherically symmetric encapsulated acoustic antibubbles. *Hydroacoustics* **2016**, *19*, 197–208.
60. Shamloo, A.; Boodaghi, M. Design and simulation of a microfluidic device for acoustic cell separation. *Ultrasonics* **2018**, *84*, 234–243. [[CrossRef](#)] [[PubMed](#)]
61. Leighton, T.G. *The Acoustic Bubble*; Academic: London, UK, 1994.
62. Shi, J.; Ahmed, D.; Mao, X.; Lin, S.C.S.; Lawit, A.; Huang, T.J. Acoustic tweezers: Patterning cells and microparticles using standing surface acoustic waves (SSAW). *Lab Chip* **2009**, *9*, 2890–2895. [[CrossRef](#)] [[PubMed](#)]
63. Dayton, P.A.; Morgan, K.E.; Klibanov, A.L.; Brandenburger, G.; Nightingale, K.R.; Ferrara, K.W. A preliminary evaluation of the effects of primary and secondary radiation forces on acoustic contrast agents. *IEEE Trans. Ultrason. Ferroelectr. Freq. Control* **1997**, *44*, 1264–1277. [[CrossRef](#)]
64. Duckhouse, H.; Mason, T.J.; Phull, S.S.; Lorimer, J.P. The effect of sonication on microbial disinfection using hypochlorite. *Ultrason. Sonochem.* **2004**, *11*, 173–176. [[CrossRef](#)] [[PubMed](#)]
65. Trampuz, A.; Piper, K.E.; Hanssen, A.D.; Osmon, D.R.; Cockerill, F.R.; Steckelberg, J.M.; Patel, R. Sonication of explanted prosthetic components in bags for diagnosis of prosthetic joint infection is associated with risk of contamination. *J. Clin. Microbiol.* **2006**, *44*, 628–631. [[CrossRef](#)] [[PubMed](#)]
66. Selman, G.G.; Jurand, A. An electron microscope study of the endoplasmic reticulum in Newt notochord cells after disturbance with ultrasonic treatment and subsequent regeneration. *J. Cell Biol.* **1964**, *20*, 175–183. [[CrossRef](#)] [[PubMed](#)]
67. Macintosh, I.J.C.; Davey, D.A. Chromosome aberrations induced by an ultrasonic fetal pulse detector. *Br. Med. J.* **1970**, *4*, 92–93. [[CrossRef](#)] [[PubMed](#)]
68. Ravitz, M.J.; Schnitzler, R.M. Morphological changes induced in the frog semitendinosus muscle fiber by localized ultrasound. *Exp. Cell Res.* **1970**, *60*, 78–85. [[CrossRef](#)]
69. Miller, M.W.; Voorhees, S.M.; Carstensen, E.L.; Eames, F.A. An histological study of the effect of ultrasound on growth of *Vicia faba* roots. *Radiat. Bot.* **1974**, *14*, 201–206. [[CrossRef](#)]
70. Miller, M.W. Comparison of micronuclei induction for X-ray and ultrasound exposures of *Vicia faba* root meristem cells. *Ultrasound Med. Biol.* **1978**, *4*, 267. [[CrossRef](#)]
71. Miller, D.L. Cell death thresholds in *Elodea* for 0.45–10 MHz ultrasound compared to gas-body resonance theory. *Ultrasound Med. Biol.* **1979**, *5*, 351–357. [[CrossRef](#)]
72. Miller, D.L. A cylindrical-bubble model for the response of plant-tissue gas bodies to ultrasound. *J. Acoust. Soc. Am.* **1979**, *65*, 1313–1321. [[CrossRef](#)]
73. Dyer, H.J.; Nyborg, W.L. Ultrasonically-induced movements in cells and cell models. *IRE Trans. Med. Electron.* **1960**, 163–165. [[CrossRef](#)]
74. Gershoy, A.; Nyborg, W.L. Perturbation of plant-cell contents by ultrasonic micro-irradiation. *J. Acoust. Soc. Am.* **1973**, *54*, 1356–1367. [[CrossRef](#)]
75. Trenchard, P.M. Ultrasound-induced orientation of discoid platelets and simultaneous changes in light transmission: preliminary characterisation of the phenomenon. *Ultrasound Med. Biol.* **1987**, *13*, 183–195. [[CrossRef](#)]
76. Williams, A.R.; Sykes, S.M.; O'Brien, W.D., Jr. Ultrasonic exposure modifies platelet morphology and function in vitro. *Ultrasound Med. Biol.* **1977**, *2*, 311–317. [[CrossRef](#)]
77. Miller, M.W.; Azadniv, M.; Doida, Y.; Brayman, A.A. Effect of a stabilized microbubble contrast agent on CW ultrasound induced red blood cell lysis in vitro. *Echocardiogr. J.* **1995**, *12*, 1–11. [[CrossRef](#)]
78. Liu, J.; Lewis, T.N.; Prausnitz, M.R. Non-invasive assessment and control of ultrasound-mediated membrane permeabilization. *Pharm. Res.* **1998**, *15*. [[CrossRef](#)]

79. Tachibana, K.; Uchida, T.; Ogawa, K.; Yamashita, N.; Tamura, K. Induction of cell-membrane porosity by ultrasound. *Lancet* **1999**, *353*, 1409. [[CrossRef](#)]
80. Belgrader, P.; Hansford, D.; Kovacs, G.T.A.; Venkateswaran, K.; Mariella, R., Jr.; Milanovich, F.; Nasarabadi, S.; Okuzumi, M.; Pourahmadi, F.; Northrup, M.A. A minisonicator to rapidly disrupt bacterial spores for DNA analysis. *Anal. Chem.* **1999**, *71*, 4232–4236. [[CrossRef](#)] [[PubMed](#)]
81. Taylor, M.T.; Belgrader, P.; Furman, B.J.; Pourahmadi, F.; Kovacs, G.T.A.; Northrup, M.A. Lysing bacterial spores by sonication through a flexible interface in a microfluidic system. *Anal. Chem.* **2001**, *73*, 492–496. [[CrossRef](#)] [[PubMed](#)]
82. Ashush, H.; Rozenszajn, L.A.; Blass, M.; Barda-Saad, M.; Azimov, D.; Radnay, J.; Zipori, D.; Rosenschein, U. Apoptosis induction of human myeloid leukemic cells by ultrasound exposure. *Cancer Res.* **2000**, *60*, 1014–1020. [[PubMed](#)]
83. Taniyama, Y.; Tachibana, K.; Hiraoka, K.; Namba, T.; Yamasaki, K.; Hashiya, N.; Aoki, M.; Ogihara, T.; Yasufumi, K.; Morishita, R. Local delivery of plasmid DNA into rat carotid artery using ultrasound. *Circulation* **2002**, *105*, 1233–1239. [[CrossRef](#)] [[PubMed](#)]
84. Lagneaux, L.; Delforge, A.; Dejeneffe, M.; Massy, M.; Moerman, C.; Hannecart, B.; Canivet, Y.; Lepeltier, M.F.; Bron, D. Ultrasonic low-energy treatment: A novel approach to induce apoptosis in human leukemic cells. *Exp. Hematol.* **2002**, *30*, 1293–1301. [[CrossRef](#)]
85. Li, G.; Xiao, H.; Glo, M.; Cheg, J. Miniaturized cell lysis device using spherically focused ultrasound. *Tsinghua Sci. Technol.* **2003**, *8*, 487–492.
86. Song, Y.; Hahn, T.; Thompson, I.P.; Mason, T.J.; Preston, G.M.; Li, G.; Paniwnyk, L.; Huang, W.E. Ultrasound-mediated DNA transfer for bacteria. *Nucleic Acids Res.* **2007**, *35*, e129-1–e129-9. [[CrossRef](#)] [[PubMed](#)]
87. Yoshida, T.; Kondo, T.; Ogawa, R.; Feril, L.B.; Zhao, Q.L.; Watanabe, A.; Tsukada, K. Combination of doxorubicin and low-intensity ultrasound causes a synergistic enhancement in cell killing and an additive enhancement in apoptosis induction in human lymphoma U937 cells. *Cancer Chemother. Pharmacol.* **2008**, *61*, 559–567. [[CrossRef](#)] [[PubMed](#)]
88. Monsen, T.; Lövgren, E.; Widerström, M.; Wallinder, L. In vitro effect of ultrasound on bacteria and suggested protocol for sonication and diagnosis of prosthetic infections. *J. Clin. Microbiol.* **2009**, *47*, 2496–2501. [[CrossRef](#)] [[PubMed](#)]
89. Drakopoulou, S.; Terzakis, S.; Fountoulakis, M.S.; Mantzavinos, D.; Manios, T. Ultrasound-induced inactivation of gram-negative and gram-positive bacteria in secondary treated municipal wastewater. *Ultrason. Sonochem.* **2009**, *16*, 629–634. [[CrossRef](#)] [[PubMed](#)]
90. Kotopoulis, S.; Schommartz, A.; Postema, M. Sonic cracking of blue-green algae. *Appl. Acoust.* **2009**, *70*, 1306–1312. [[CrossRef](#)]
91. Zhang, G.; Zhang, P.; Liu, H.; Wang, B. Ultrasonic damages on cyanobacterial photosynthesis. *Ultrason. Sonochem.* **2006**, *13*, 501–505. [[CrossRef](#)] [[PubMed](#)]
92. Furusawa, Y.; Fujiwara, Y.; Campbell, P.; Zhao, Q.L.; Ogawa, R.; Hassan, M.A.; Tabuchi, Y.; Takasaki, I.; Takahashi, A.; Kondo, T. DNA double-strand breaks induced by cavitation mechanical effects of ultrasound in cancer cell lines. *PLoS ONE* **2012**, *7*, e29012. [[CrossRef](#)] [[PubMed](#)]
93. Hassan, M.A.; Ahmed, I.S.; Campbell, P.; Kondo, T. Enhanced gene transfection using calcium phosphate co-precipitates and low-intensity pulsed ultrasound. *Eur. J. Pharm. Sci.* **2012**, *47*, 768–773. [[CrossRef](#)] [[PubMed](#)]
94. Ly, M.; Lu, F.; Maheshwari, G.; Subramanian, S. Microscale acoustic disruption of mammalian cells for intracellular product release. *J. Biotechnol.* **2014**, *184*, 146–153. [[CrossRef](#)] [[PubMed](#)]
95. Samal, A.B.; Adzerikho, I.D.; Mrochek, A.G.; Loiko, E.N. Platelet aggregation and change in intracellular Ca²⁺ induced by low frequency ultrasound in vitro. *Eur. J. Ultrasound* **2000**, *11*, 53–59. [[CrossRef](#)]
96. Zourob, M.; Hawkes, J.J.; Coakley, W.T.; Treves Brown, B.J.; Fielden, P.R.; McDonnell, M.B.; Goddard, N.J. Optical leaky waveguide sensor for detection of bacteria with ultrasound attractor force. *Anal. Chem.* **2005**, *77*, 6163–6168. [[CrossRef](#)] [[PubMed](#)]
97. Mizrahi, N.; Zhou, E.H.; Lenormand, G.; Krishnan, R.; Weihs, D.; Butler, J.P.; Weitz, D.A.; Fredberg, J.J.; Kimmel, E. Low intensity ultrasound perturbs cytoskeleton dynamics. *Soft Matter* **2012**, *8*, 2438–2443. [[CrossRef](#)] [[PubMed](#)]

98. Hawkes, J.J.; Limaye, M.S.; Coakley, W.T. Filtration of bacteria and yeast by ultrasound-enhanced sedimentation. *J. Appl. Microbiol.* **1997**, *82*, 39–47. [[CrossRef](#)] [[PubMed](#)]
99. Mazzawi, N.; Postema, M.; Kimmel, E. Bubble-like response of living blood cells and microparticles in an ultrasound field. *Acta Phys. Pol. A* **2015**, *127*, 103–105. [[CrossRef](#)]
100. Ding, X.; Peng, Z.; Lin, S.C.S.; Geri, M.; Li, S.; Li, P.; Chen, Y.; Dao, M.; Suresh, S.; Huang, T.J. Cell separation using tilted-angle standing surface acoustic waves. *Proc. Natl Acad. Sci. USA* **2014**, *111*, 12992–12997. [[CrossRef](#)] [[PubMed](#)]
101. Li, P.; Mao, Z.; Peng, Z.; Zhou, L.; Chen, Y.; Huang, P.H.; Truica, C.I.; Drabick, J.J.; El-Deiry, W.S.; Dao, M.; et al. Acoustic separation of circulating tumor cells. *Proc. Natl Acad. Sci. USA* **2015**, *112*, 4970–4975. [[CrossRef](#)] [[PubMed](#)]
102. Walther, T.; Postema, M. Device for the Identification, Separation and/or Cell Type-Specific Manipulation of at Least One Cell of a Cellular System. U.S. Patent 14476187, 3 September 2014.
103. Pitt, W.G.; Ross, S.A. Ultrasound increases the rate of bacterial cell growth. *Biotechnol. Prog.* **2003**, *19*, 1038–1044. [[CrossRef](#)] [[PubMed](#)]
104. Raz, D.; Zaretsky, U.; Einav, S.; Elad, D. Cellular alterations in cultured endothelial cells exposed to therapeutic ultrasound irradiation. *Endothelium* **2005**, *12*, 201–213. [[CrossRef](#)] [[PubMed](#)]
105. Hultström, J.; Manneberg, O.; Dopf, K.; Hertz, H.M.; Brismar, H.; Wiklund, M. Proliferation and viability of adherent cells manipulated by standing-wave ultrasound in a microfluidic chip. *Ultrasound Med. Biol.* **2007**, *33*, 145–151. [[CrossRef](#)] [[PubMed](#)]
106. Zderic, V.; Clark, J.I.; Vaezy, S. Drug delivery into the eye with the use of ultrasound. *J. Ultrasound Med.* **2004**, *23*, 1349–1359. [[CrossRef](#)] [[PubMed](#)]
107. Or, M.; Kimmel, E. Modeling linear vibration of cell nucleus in low intensity ultrasound field. *Ultrasound Med. Biol.* **2009**, *35*, 1015–1025. [[CrossRef](#)] [[PubMed](#)]
108. Frenkel, V.; Kimmel, E.; Iger, Y. Ultrasound-facilitated transport of silver chloride (AgCl) particles in fish skin. *J. Control. Release* **2000**, *68*, 251–261. [[CrossRef](#)]
109. Mazzawi, N.; Kimmel, E.; Tsarfaty, I. The effect of low-intensity ultrasound and met signaling on cellular motility and morphology. *Appl. Acoust.* **2019**, *143*, 1–6. [[CrossRef](#)]



© 2018 by the authors. Licensee MDPI, Basel, Switzerland. This article is an open access article distributed under the terms and conditions of the Creative Commons Attribution (CC BY) license (<http://creativecommons.org/licenses/by/4.0/>).